

## MECHANICAL PROPERTIES FOR FRACTURE ANALYSIS OF MILD STEEL STORAGE TANKS

**R. L. Sindelar, P. S. Lam, G. R. Caskey, Jr.**  
Savannah River Technology Center  
Westinghouse Savannah River Company  
Aiken, South Carolina

**L. Y. Woo**  
Georgia Institute of Technology  
Atlanta, Georgia

### ABSTRACT

Mechanical properties of 1950's vintage, A285 Grade B carbon steels have been compiled for elastic-plastic fracture mechanics analysis of storage tanks (Lam and Sindelar, 1999). The properties are from standard Charpy V-notch (CVN), 0.4T planform Compact Tension (C(T)), and Tensile (T) specimens machined from archival steel from large water piping. The piping and storage tanks were constructed in the 1950s from semi-killed, hot-rolled carbon steel plate specified as A285 Grade B. Evaluation of potential aging mechanisms at both service conditions shows no loss in fracture resistance of the steel in either case.

Site and literature data show that the A285, Grade B steel, at and above approximately 70°F, is in the upper transition to upper shelf region for absorbed energy and is not subject to cleavage cracking or a brittle fracture mode. Furthermore, the tank sidewalls are 1/2 or 5/8-inch thick, and therefore, the J-resistance ( $J_R$ ) curve that characterizes material resistance to stable crack extension under elastic-plastic deformation best defines the material fracture toughness. The  $J_R$  curves for several heats of A285, Grade B steel tested at 40°F, a temperature near the average ductile-to-brittle (DBTT) transition temperature (CVN @ 15 ft-lb), are presented. This data is applicable to evaluate flaw stability of the storage tanks that are operated above 70°F since, even at 40°F, crack advance is observed to proceed by ductile tearing.

### INTRODUCTION

Mild carbon steel with specification ASTM A285 is a common material of construction for vessels in the petroleum and nuclear industries. Storage tanks were constructed between 1951 and 1956 from hot-rolled carbon steel plate specified as ASTM A285 Grade B. Extensive analyses and experimental investigations

have demonstrated tank integrity in full consideration of potential service-induced degradation mechanisms, including stress corrosion cracking (Marra, et. al., 1995).

The operating temperature of the storage tanks is 70°F and above, placing the carbon steel in the upper transition region where ductile tearing would be the failure mode. The Department of Energy (DOE) Tank Structural Integrity Panel has recommended  $J_R$  Analysis or Deformation Plasticity Failure Analysis Diagrams as elastic-plastic fracture mechanics (EPFM) analysis tools to evaluate integrity of storage tanks (Bandyopadhyay, et al., 1997). The approach allows determination of critical flaw size under conditions where stable crack extension would precede a ductile tearing instability. A J-integral fracture mechanics analysis has been performed to evaluate flaw stability using material  $J_R$  curves to characterize the fracture toughness and to set the criterion for a cut-off to the  $J_R$  curve (Lam and Sindelar, 1999).

The validity and limitations of the fracture mechanics analysis depend, in part, upon the available mechanical property data. The steel suppliers provided tensile properties for each heat of steel that was used in construction of the tanks. Impact properties were measured for one sample of this steel only. Fracture mechanics analyses require measurement of fracture toughness. Procedures had not been established in the early 1950's to measure fracture toughness; therefore,  $J_R$  curves are not available for the specific heats of steel in the storage tanks. However,  $J_R$  curves for fracture toughness have been measured on specimens of carbon steel pipe that were made from plates in the 1950's to the same specifications as the storage tanks. The application of this combined database to analysis of the storage tanks has been demonstrated through fundamental materials understanding described in this report. Limitations to the application of this data have been identified and additional fracture tests proposed to address the limitations.

## **EVALUATION OF 1950'S VINTAGE A285, GRADE B CARBON STEEL IN STORAGE TANKS AND PIPING**

The storage tanks and the cooling water piping were constructed of ASTM A285, Grade B carbon steel during the 1950s. Based on evaluation of the composition, fabrication, and service conditions of the storage tanks and cooling water piping, the mechanical property data from the pipe sections are judged to be applicable to analysis of the storage tanks.

### **Composition**

#### Storage Tanks

The carbon steel conformed to specification ASTM A285-50T, Grade B firebox quality (see Table 1) including the 7/8-inch plates that form the bottom knuckle region of one of the two tank types. The average, maximum, and minimum constituents reported for 21 heats of the steel are listed in Table 2. The material was melted in an open-hearth furnace, semi-killed, and then hot rolled into plate.

#### Piping

Large diameter piping was built to a 1950's edition of the ASME, Section VIII, Unfired Pressure Vessel Code. Portions of the piping system that were fabricated from A285 carbon steel were removed for mechanical testing. Table 3 shows the composition of four different heats of steel and two weldments.

The compositions of the steels in the piping are also within the specifications for ASTM A285-50T, Grade B. The carbon contents of the pipe steels correspond to the most frequently occurring carbon contents in the tank steels, 0.10 – 0.14 wt % carbon, but do not cover five of the 21 heats of steel with carbon contents in the range 0.15 to 0.20 wt %. On average the manganese contents in the piping steels are slightly higher than in the tank steels leading to higher manganese carbon ratios for the pipe steels. The manganese carbon ratios for the tank steels have a bimodal distribution with peaks at 3.8 and 4.6 Mn/C. The manganese carbon ratios for the pipe steel correspond to the higher peak at 4.6. Overall, the sections of pipe steel most closely resemble those tank steels with lower carbon and higher manganese to carbon ratios.

### **Fabrication**

#### Storage Tanks

Tank construction conformed to the Rules for Construction of Unfired Pressure Vessels, Section VIII of the ASME Boiler Construction Code 1949 or 1952. Welding procedures and welding operator qualifications were in compliance with Section IX of the ASME Code.

The wall thickness of the steel plates in the tanks were: 1/2-inch for top and bottom plates; 1/2- or 5/8-inch for side plates; 1/2- or 7/8-inch for knuckle plates joining the bottom and sides.

Tank inspections included visual, radiographic, and leak testing. All welds were visually inspected upon completion of the weld and/or after each pass if requested. The welds had to be approved before radiographic inspection could begin. All welds affecting the ability of the tank to retain liquids or gasses were radiographed by methods that met the accuracy required by the Code. This included welds to and in manholes, nozzles, sleeves, or couplings attached to or penetrating the steel shell. All repaired welds were radiographed.

#### Piping

The large diameter piping had a wall thickness of 0.5 inch. It is assumed that the pipe was fabricated by roll forming and seam welding. Sections of piping were joined by butt welds made by shielded metal-arc welding with AWS E6010 electrodes welding from the outside of the pipe, back gouging, and then rewelding from the inside of the pipe. Radiographic inspections were not performed on the original pipe welds and were not required by any of the applicable piping standards at the time of construction.

### **Service Conditions and Effects of Service on Mechanical Properties**

A potential difference between the storage tanks and cooling water piping is in the exposure of the materials to service conditions that could potentially affect the mechanical properties of the A285 Grade B carbon steel. Several degradation mechanisms that potentially could affect either the mechanical properties of the steel or the load bearing capacity of the tanks have been identified. These are: corrosion (general and pitting); thermal embrittlement; radiation embrittlement; and hydrogen embrittlement. They have been evaluated (Marra et. al., 1995 and Bandyopadhyay, et. al., 1997) and a summary of the results is below.

#### Corrosion

In-service inspection and laboratory testing have shown that general corrosion and pitting are insignificant. Ultrasonic inspections of the tank walls indicated that no detectable thinning had occurred in over 25 years of operation. In addition, corrosion coupons immersed in the tanks for approximately 15 years showed little evidence of general corrosion. Likewise, no significant pitting has occurred. Only broad, shallow pitting has been observed. Shallow pitting would have insignificant effects on the mechanical properties of the material.

#### Thermal Embrittlement

Both elevated and low temperature environments may result in the embrittlement of carbon steels. Embrittlement is characterized by an increase in the strength and hardness of the material with a corresponding loss in ductility and toughness.

**Table 1 - ASTM Requirements for Chemical Composition for A285-50T, Grade B Firebox Quality**

For plates ≤ 0.75" thickness	Composition, wt. %			
	C max	Mn max	P max	S max
	0.2	0.8	0.035	0.04

**Table 2 - Chemical Composition of Storage Tank Plates**

	Composition, wt. %			
	C	Mn	P	S
Average Composition of 21 Heats	0.12	0.48	0.01	0.028
Maximum Composition from 21 Heats	0.20	0.58	0.015	0.037
Minimum Composition from 21 Heats	0.08	0.37	0.007	0.020

**Table 3 - Composition of Material from Cooling Water Piping**

Material	Specimen ID	Composition, wt%					
		C	Mn	P	S	Si	Cu
A285 Pipe	P5	0.14, 0.14a, 0.148b	0.56 0.56a	0.006 0.007a	0.029 0.073a	0.09 0.063a	0.045 0.047a
A285 Pipe	P6	0.12	0.56	0.007	0.020	0.12	0.096
A285 Pipe	P7	0.12	0.54	0.007	0.027	0.11	0.170
A285 Pipe	P8	0.10	0.58	0.006	0.027	0.10	0.100
A285 Weld	CW11	0.09	0.56	0.008	0.015	0.14	0.095
A285 Weld	CW12	0.09	0.54	0.008	0.017	0.13	0.100

**Notes:**

1. The composition reported from wet chemistry analysis in 1983
2. <sup>a</sup>1998 Analysis Using Wavelength Dispersive X-Ray Fluorescence Spectroscopy (WDS). The WDS analysis also included Ni (0.032 %), Cr (0.030%), and Mo (0.003%)
3. <sup>b</sup>1998 Analysis Using Carbon Analyzer

The temperatures experienced by the storage tanks (measured temperatures of 84 to 146°F) are well below those needed for elevated temperature embrittlement (200-500°F) and above those needed for low temperature embrittlement (DBTT). Therefore, thermal embrittlement is not considered to be a significant degradation mechanism.

Radiation Embrittlement

Radiation embrittlement of the ferritic steels such as the carbon steels of the storage tanks arises from displacement of atoms in the steel by neutron irradiation or exposure to high-energy gamma radiation. The embrittlement is characterized as a reduction in ductility and/or an increase in the ductile to brittle transition temperature with a loss in upper shelf absorbed energy, as measured by standard CVN testing.

The highest estimated damage level in a storage tank is less than 4.0E-7 dpa and is well below the level of 1.0E-5 dpa where

changes in the mechanical properties of ferritic steels due to radiation damage have been observed.

Hydrogen Embrittlement

Hydrogen embrittlement of carbon steel may occur through formation of methane gas from radiolytically or cathodically produced hydrogen that diffuses into the steel and reacts with the carbon. The reaction results in severe loss of ductility and strength for the steel. However, data from the American Petroleum Institute demonstrates that carbon steel at temperatures less than 500°F (260°C) and pressures less than several hundred atmospheres can perform safely for an indefinite time (API, 1977). Since operating temperatures and pressures in the tanks are well within the parameters, the mechanism is insignificant.

None of the degradation mechanisms significantly affect the mechanical properties of the A285 steel in storage tank service.

This conclusion also applies to the pipe service since the piping carried cooling water at temperatures ranging from 40°F to 180°F (4.4°C to 82.2°C), and at pressures ranging up to 70 psig. Therefore, considering the composition, fabrication, and service conditions of the A285 steel, the properties of A285 steel from the piping are applicable to the tanks.

## MECHANICAL PROPERTY DATA OF A285, GRADE B MATERIAL

The tanks operate above a minimum temperature of 70°F in order to avoid the potential for brittle fracture. This temperature corresponds to upper transition to upper shelf behavior for A285 steel and thus failure could only occur through ductile tearing. Elastic-plastic analysis must be used to characterize the deformation of the thin wall tanks. The J-resistance ( $J_R$ ) curve that characterizes material resistance to stable crack extension under elastic-plastic deformation is used to define the material fracture toughness.

A database is being developed to quantify the fracture toughness and provide a statistical base for flaw stability analysis. The initial data available for the database is from testing of A285 carbon steel from the cooling water piping performed by Materials Engineering Associates, Inc. Specimens were machined from four pieces of pipe and two weld regions. The mechanical properties of the archival A285 carbon steel were characterized through the following tests:

1. Static and dynamic tensile
2. Static and dynamic compact tension fracture toughness 0.4 C(T)
3. Charpy V Notch

The specimens were oriented in either the L-C orientation or the C-L orientation. The L-C orientation positioned the crack plane perpendicular to the rolling direction, while C-L orientation positioned the plane parallel to the rolling direction. Both the tensile test and fracture toughness tests were conducted with all specimens in the L-C orientation. The Charpy V Notch test was conducted in both orientations. The specimen orientations are illustrated in Figure 1.

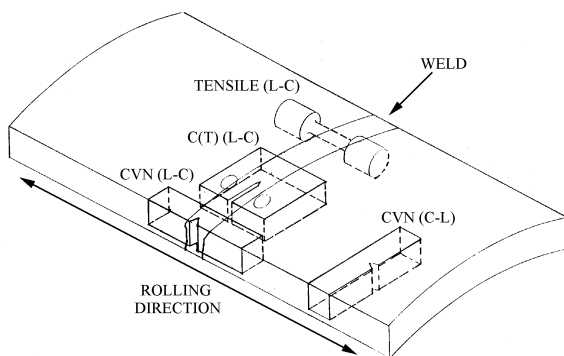


Figure 1 – Orientation of Test Specimens

Static and dynamic tests accounted for normal and seismic loads. The dynamic loading rates for the material were too high

compared to the rates expected in the tanks under seismic conditions and therefore the results of the static testing only are provided in the following sections.

## Tensile Properties

### Storage Tanks

The ASTM specification A285-50T for the tensile properties of A285, Grade B steel is shown in Table 4 below. ASTM Standard A20-50 specified tensile specimens with an 8-inch gauge length machined with their axes parallel to the longitudinal direction of the plate. The range of values from triplicate tests of the 21 heats of steel from tank construction are within the ASTM specification for yield strength, tensile strength, and elongation.

### Piping

The testing was in accordance with ASTM E8 specification for tension testing of metallic materials with the subsize tensile specimen, 0.25-inch diameter. The results of the static tensile tests are summarized in Table 5. All specimens were in the L-C orientation and were tested at 40°F (4.4°C), the minimum service temperature for the pipe.

The tensile specimens for the weld material were machined so that the gage section contained base, heat-affected-zone, and weld metal. All failures of these specimens occurred in the base metal. Therefore, neither the weld metal nor the heat-affected-zone is the weak link in the weld area.

## Fracture Properties

Fracture of carbon steels may occur by ductile rupture or microvoid coalescence, by brittle or cleavage fracture, or by ductile tearing interrupted by brittle fracture. Decreasing temperature, increasing constraint, and rapid loading rate promote brittle fracture. The transition from ductile to brittle fracture is also a material property that depends on grain size and composition of the steel, as discussed later.

### Storage Tanks

Fracture characteristics of the A285 carbon steel used in construction of the tanks were investigated after construction to evaluate the susceptibility of the steel to brittle fracture and establish temperature limits for operation of the tanks. The nil-ductility transition temperature (NDTT) was  $-20 \pm 10^\circ\text{F}$  as measured by the ASTM E-208 Drop Weight Test with 0.5-inch thick non-standard type P-2 specimens.

Charpy V-Notch (CVN) specimens were machined from an archival plate of A285 steel from the construction of the tanks and tested over the temperature range  $-30$  to  $+111^\circ\text{F}$ . The ductile-to-brittle transition temperature (DBTT), the temperature at 15 ft-lb absorbed energy, was  $+45^\circ\text{F}$  and the upper shelf energy impact energy was estimated at 62 ft-lb. The orientation of the test specimens with respect to the plate rolling direction was not reported. Based on the relatively low upper shelf

energy impact energy (USE), the CVN specimens were probably in the T-L orientation.

An extensive database of absorbed energy from Charpy V-notch testing is reported in the literature for A285, Grade C steel (Hamel, 1958). Data applicable to the storage tanks can be developed by using the 33 data in which the grain size is greater or equal to ASTM number 6 and carbon content is less than or equal to 0.22 wt.%. The range in DBTT is -35 to 60°F and the average is 27°F. This data is consistent with the site-specific tank plate steels and the piping steels.

### Piping

Charpy V-notch testing was also performed using the four heats of plate material and two weld materials. The results shown in Table 6 are consistent with the literature results and the tank plate materials.

Fracture toughness specimens of the piping steel were machined to the ASTM E399 configuration for a specimen with thickness equal to 0.394 inch. The tests were in accordance with the applicable portions of ASTM E813 specification, the standard test method for  $J_{Ic}$ . All specimens were pre-cracked in accordance with ASTM E399 requirements.

Static fracture toughness tests were conducted at a stress intensity rate of 40 ksi  $\sqrt{\text{in}}$  /min; the results are summarized in Table 7. Testing occurred at 40°F (4.4°C) with all specimens in the L-C orientation. All fractures were ductile over the entire crack extension range except for weld specimen CW11-2 where fracture began and continued in a ductile manner but changed to cleavage after significant crack extension. The tests did not meet the validity requirements of ASTM E-813 because of the ductility of the steel.

The results of the static 0.4 C(T) tests provided fracture properties in the form of J-resistance or J-R curves. J is the energy made available at the crack tip per unit crack extension ( $\Delta a$ ). The calculated value of J was a modified J ( $J_m$ ), where  $J_m$  was the deformation theory J ( $J_d$ ) adjusted by a term that accounted for the elastic plastic failure. For small crack extensions on the order of 1mm,  $J_m$  was equal to  $J_d$ . However, at larger crack extensions the difference between the two J values was significant with  $J_m$  believed to produce values that were more geometry independent. Therefore, the modified J was used for all static tests.

$J_{Ic}$  is the energy at the onset of crack initiation and was calculated from the power law equation at a fixed crack extension of 0.2 mm. The value of the fixed crack extension was chosen based on past experience and approximates the maximum blunting extension attainable with low strength structural steels. Using the value for  $J_{Ic}$ , the elastic initiation fracture toughness  $K_{Ic}$  may be calculated from the following equation:

$$K_{Ic} = \left[ \frac{E \cdot J_{Ic}}{(1 - \nu^2)} \right]^{0.5}$$

where  $\nu = 0.3$  and  $E = 3 \times 10^7$ . The values for  $K_{Ic}$  are shown in Table 7. The average toughness for the pipe material was 205 ksi $\sqrt{\text{in}}$  with a standard deviation of 42 ksi $\sqrt{\text{in}}$ . For the weld material, the average toughness was 148.5 ksi $\sqrt{\text{in}}$  with a standard deviation of 7.8 ksi $\sqrt{\text{in}}$ .

The  $J_m$  vs.  $\Delta a$  curves under static loading conditions are shown in Figure 2. The data was fit to a power law equation of the form,  $J = C (\Delta a)^n$  where C and n are constants. The values of C and n are listed in Table 8.

### SEM and Optical Microscopy

Fracture surfaces of four compact tension specimens were examined: two static pipe specimens (P5-2 and P8-2), one static weld specimen (CW11-2), and one dynamic pipe specimen (P6-8). The surfaces were inspected for evidence of ductile or brittle fracture.

The ductile nature of the crack growth is evident in the optical photograph (upper left) and the electron micrographs in Figure 5 of specimen P5-2. The optical photograph shows plastic deformation or lateral contraction of the specimen in the region of crack advance ( $\Delta a$ ). The high magnification electron micrographs show dimpled rupture or microvoid coalescence, a characteristic of ductile failure. The only indication of brittle fracture was seen in the dynamic fracture specimen, where a transition from ductile to cleavage fracture was beginning in the region of maximum crack extension.

### **Dependency of Mechanical Properties on Material and Test Conditions**

Several material or test condition parameters are identified that can affect the mechanical properties of the A285 steel and the applicability of the pipe material test results to analysis of the storage tanks.

#### Effects of Composition on Tensile Properties

Carbon and manganese are the main compositional variables that influence the tensile properties, yield strength, tensile strength, and ductility of A285 carbon steel. Both carbon and manganese raise the strength and lower the ductility of hot rolled carbon steel. However, the reported elongations of the tank and pipe steels can not be compared because the measured elongation is sensitive to the shape of the tensile specimen and its gauge length. The tensile specimens for the pipe steel were sub-sized round bar specimens, whereas the tensile specimens for the tank steels were flat specimens with an 8-inch gauge length, which was the standard test specimen in the early and mid 1950s.

The carbon contents of the 21 heats of carbon steel in the storage tanks range from 0.08 to 0.20 wt.% carbon with 14 of the 21 analyses in the range of 0.09 to 0.14 wt.% carbon. The four sections of piping also have carbon analyses within this latter range. The manganese to carbon ratios for the tank steels range from less than 2.6 to 5.8 and have a bimodal distribution with

**Table 4 - ASTM Requirements for Tensile Properties for A285-50T, Grade B Firebox Quality**

For plates ≤ 0.75” in thickness	Mechanical Property Ranges		
	Tensile (ksi)	Yield (ksi)	% Elongation in 8-inches
	50-60	27	27

**Table 5- Static Tensile Test Data Summary for A285 Carbon Steel from the Cooling Water Piping**

Material	Specimen ID	Yield Stress			Ultimate Stress (ksi)	Elongation (%)	Reduction In Area (%)
		Upper (ksi)	Lower (ksi)	0.2 % (ksi)			
A285 Pipe	P5-2	43.0	36.6	37.1	58.0	39.2	70.0
A285 Pipe	P6-2	38.3	34.7	35.6	57.8	39.6	70.4
A285 Pipe	P7-2	42.8	35.6	35.9	59.6	37.8	63.1
A285 Pipe	P8-2	43.4	36.8	37.5	57.8	39.4	62.8
A285 Weld	CW11-2	47.9	43.8	45.0	62.8	35.5	66.8
A285 Weld	CW12-2	49.4	46.5	47.2	63.5	23.0	66.8

Note: Static loading rate approximately  $1 \times 10^3$  psi/sec; 40 - 80 seconds to upper yield stress

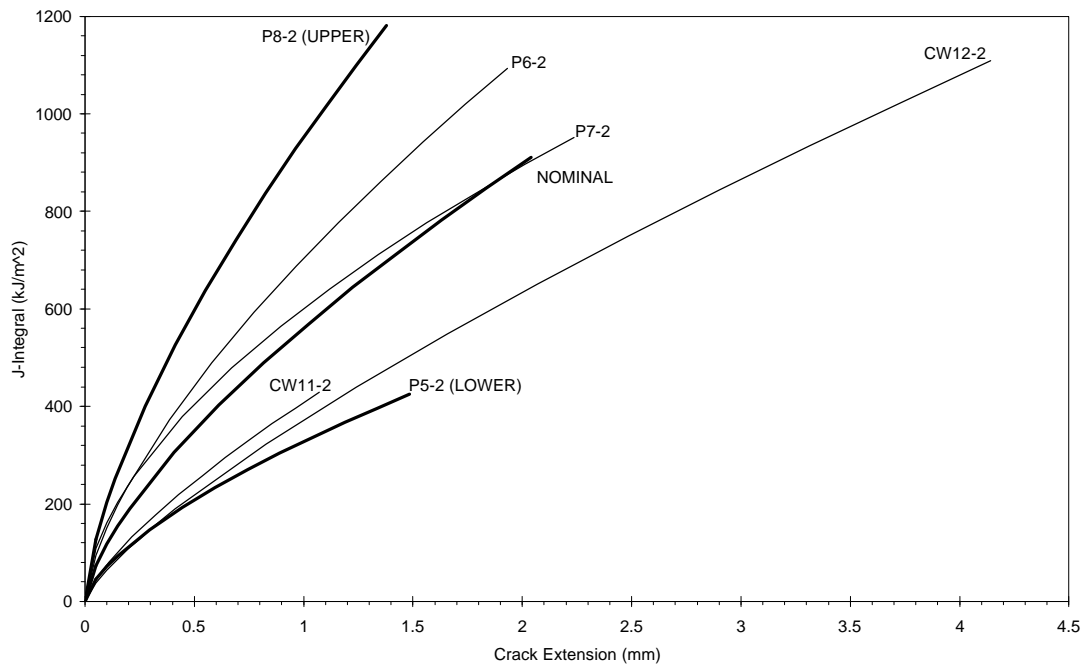


**Figure 2 - J-R Curves for A285 Grade B Steel at 40°F**

**Table 6 - Charpy V Notch Impact Test Data Summary for A285 Carbon Steel from the Cooling Water Piping**

Material	Specimen ID	41J (30 ft-lb) Temperature		Shelf Energy Level				Energy Level at 40°F	
		(°C)	(°F)	L-C orientation (J)	L-C orientation (ft-lb)	C-L orientation (J)	C-L orientation (ft-lb)	(J)	(ft-lb)
A285 Pipe	P5-2	14	57	149	110	52	38	18	13
A285 Pipe	P6-2	15	59	285	210	76	56	14	10
A285 Pipe	P7-2	1	34	230	170	65	48	54	40
A285 Pipe	P8-2	-2	28	285	210	83	61	95	70
A285 Weld	CW11-2	-8	18	127	94	N/A	N/A	72	53
A285 Weld	CW12-2	-15	5	134	99	N/A	N/A	85	63

**Table 7 - Static Fracture Toughness Data Summary for A285 Carbon Steel from the Cooling Water Piping**

Material	Specimen ID	$J_{Ic}$		$K_{Ic}$		Failure Type
		in-lb/in <sup>2</sup>	kJ/m <sup>2</sup>	ksi $\sqrt{in}$	MPa $\sqrt{m}$	
A285 Pipe	P5-2	650	113.8	146	160.9	Ductile
A285 Pipe	P6-2	1370	240	213	233.6	Ductile
A285 Pipe	P7-2	1369	239.8	212	233.5	Ductile
A285 Pipe	P8-2	1844	322.9	247	271.0	Ductile
A285 Weld	CW11-2	714	125.1	154	168.7	Ductile/Cleavage
A285 Weld	CW12-2	620	108.5	143	157.1	Ductile

Note: For both ductile and ductile/cleavage failure types, J is the value at the initial maximum load point which, on a tensile test, would correspond to the upper yield point. For cleavage failure types, J is measured at the point of cleavage.

**Table 8 – Values of C and n for the Power Law Fit to the  $J_R$  data**

Specimen Number	C (Newton/(mm) <sup>n+1</sup> )	n
P5-2	328.1	0.6578
P6-2	704.2	0.6688
P7-2	601.2	0.571
P8-2	951.5	0.6716
CW11-2	408	0.7346
CW12-2	372.8	0.7668

peaks at Mn/C ratios of 3.8 and 4.6. Manganese to carbon ratios for the piping are between 4.0 to 5.8, overlapping the higher peak in the bimodal distribution for the tank steel. As a consequence of the higher manganese contents (0.54-0.58 wt % Mn), the pipe steels have slightly higher strengths than the tank steels for the same carbon contents.

#### Effects of Composition on Impact and Fracture Toughness Properties

Carbon has been shown to raise the transition temperature and lower the upper shelf energy of carbon steels whereas manganese and silicon have the opposite effect. Consequently, the Mn/C ratio can be used as an indicator of the impact properties; fracture toughness is expected to vary with composition in the same manner.

The DBTT for the pipe was in the range of -25°F to 50°F (-32°C to 10°C), comparable to that of the tank steel (45°F).

The relation between Mn/C ratio and fracture toughness is evident in results from compact tension tests conducted at 40°F on steel from the pipe (Tables 3 & 7). The static fracture toughness increased from 650 to 1844 in-lb/in<sup>2</sup> as the Mn/C ratios increased from 4.0 to 5.8. The upper shelf energy measured in CVN tests (Table 6) shows a similar relation to the Mn/C ratio.

#### Effects of Microstructure on Fracture Toughness Properties

The ferrite grain size and volume fraction pearlite, influence the fracture of carbon steels and are controlled by the composition and finishing temperature during hot rolling. A three fold increase in ferrite grain size from  $4.6 \times 10^{-4}$  inch to  $12.1 \times 10^{-4}$  inch increased the brittle fracture transition temperature from -42°C to +17°C in a 0.11 wt% carbon steel (Burns and Pickering, 1964); a similar trend was seen in A285 Grade C steel (Hamel, 1958). Within the range of carbon content in the storage tank and cooling water pipe steels (0.08 to 0.20 wt% C), a small variation in volume fraction pearlite would be expected. The only available microstructures, from plate P7 from the pipe and a sample from in-situ metallography of a storage tank, have comparable grain sizes and volume fractions of pearlite.

#### Effects of Thickness on Fracture Toughness Properties

Constraint, which includes out-of-plane or thickness effects, has an effect on the fracture parameter value at failure and the  $J_R$  curve. For highly constrained conditions, fracture usually occurs at a lower value of the fracture parameter than for low constraint.

The C(T) specimens machined from the piping had a thickness of 0.394 inch. Since the thickness of these specimens is less than the thickness of the tank walls (0.5 or 0.625 inches), the constraint effects on the

fracture parameters needs to be considered. Research is being conducted to formulate an advanced fracture mechanics methodology (J-A2) that allows for consideration of constraint effects in ductile materials (Chao and Lam, 1998 and Chao, et. al., 1999).

The J-A2 methodology is being developed to identify fracture parameters that are independent of specimen geometry, such as crack depth and sample thickness.

#### Orientation Effects on Fracture Toughness Properties

The texture formed during hot rolling of carbon steel has a pronounced effect on the fracture toughness and impact energy. This is demonstrated in the impact tests on the pipe steel where the orientation had a significant effect on the upper shelf energy but a negligible one on the lower shelf energy. L-C specimens had an upper shelf energy three to four times greater than that for the C-L specimens. Consequently, fracture toughness at temperatures in the upper shelf region would be lower in the T-L orientation than in the L-T orientation of rolled steel plates.

#### Effects of Temperature

The lower bound temperature of the storage tanks studied is 70°F (21.1°C), which is well above both the NDT and the DBTT. At this temperature, the tank steels will exhibit upper transition to upper shelf behavior. The initial growth of structural flaws would be stable extension by ductile tearing under sufficiently high mechanical loads. Therefore, fracture analyses based on ductile failure or on elastic-plastic tearing instability criteria are applicable to storage tanks and best represent material behavior.

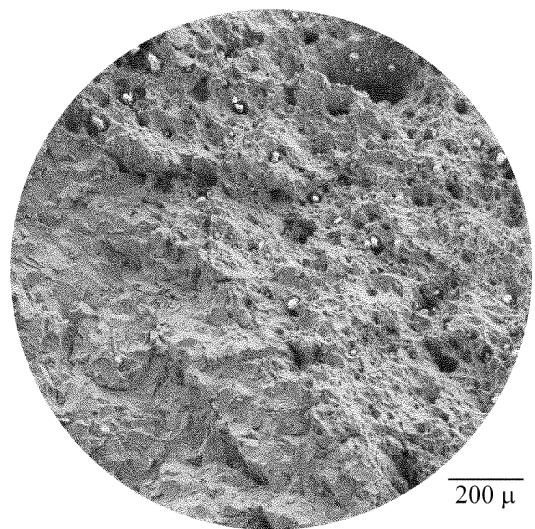
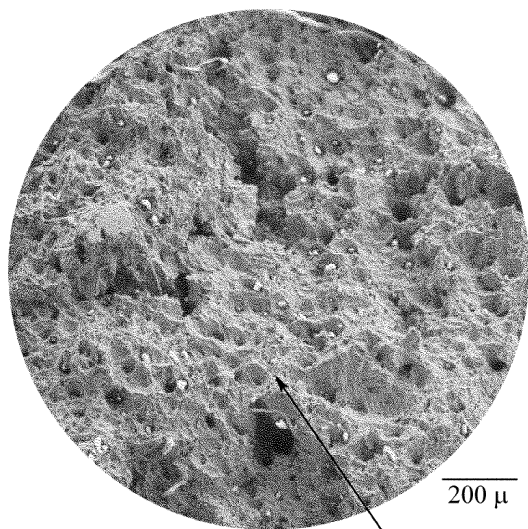
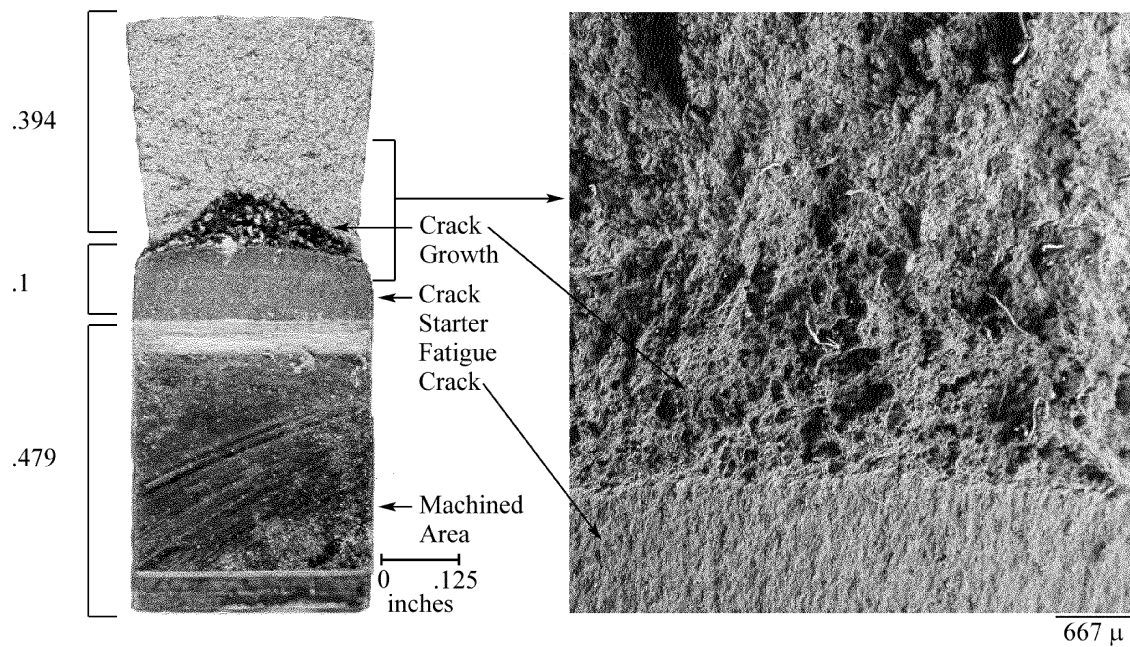
The response of A285 Grade B steel to loading at 40°F (4.4°C) is conservative when compared to the response at actual operating temperatures,  $\geq 70^\circ\text{F}$  (21.1°C). An elastic-plastic fracture analysis using the results of the 40°F (4.4°C) tests would provide a conservative estimate of flaw stability.

#### Effects of Loading Rate

The loading rate in tensile and fracture toughness testing of carbon steel affects both yield strengths and fracture toughness ( $K_{IC}$ ) values. In general, static yield strength are lower than dynamic yield strengths, and fracture toughness value of  $K_{IC}$  under dynamic loading are lower than the static values in the fracture transition temperature region. Crack resistance ( $J_R$ ) curves under dynamic loading were not developed in these tests. For seismic conditions, it is important that dynamic testing reflect the loading rate appropriate to the seismic response of the tanks.

## **CONCLUSIONS**

An initial database of elastic-plastic fracture toughness properties has been established for 1950s vintage A285,



Ductile fracture during crack growth.

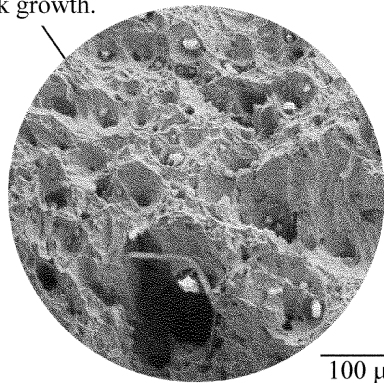


**Figure 3 – Fracture Surface of P5-2**

Grade B steel. The role of material composition, tank temperature, constraint, orientation, and loading rate effects on the mechanical properties has been presented.

## ACKNOWLEDGEMENT

Our colleague Dr. Bruce J. Wiersma is the lead investigator for service effects to the storage tanks and has provided much of the background work for this report. This research was supported in part by an appointment to the U. S. Department of Energy Scientists Emeritus Research Participation program at the Westinghouse Savannah River Company administered by the Oak Ridge Institute for Science and Education. This work was funded by the U. S. Department of Energy under contract No. DE-AC09-96SR18500.

## REFERENCES

American Petroleum Institute Report "Steels for Hydrogen Service at Elevated Temperatures and Pressures," API-941, 2<sup>nd</sup> Edition, 1977.

Bandyopadhyay, K., S. Bush, M. Kassir, B. Mather, P. Shewmon, M. Streicher, B. Thompson, D. van Rooyen, and J. Weeks, "Guidelines for Development of Structural Integrity Programs for DOE High-Level Waste Storage Tanks," BNL-52527, UC-406, prepared by Brookhaven National Laboratory for the United States Department of Energy, January 1997.

Burns, K. W. and F. B. Pickering, "Deformation and Fracture of Ferrite-Pearlite Structures," Journal of the Iron and Steel Institute, Nov. 1964, pp. 899-906.

Chao, Y. J. and P. S. Lam, "On the Use of Constraint Parameter  $A_2$  Determined from Displacement in Predicting Fracture Event," Engineering Fracture Mechanics, Vol. 61, pp. 487-502, 1998.

Chao, Y. J., X. K. Zhu, P. S. Lam, M. R. Louthan, and N. C. Iyer, "Application of Two-Parameter  $J-A_2$  Description to Ductile Crack Growth," submitted to the 31<sup>st</sup> National Symposium on Fatigue and Fracture Mechanics, June 29-July 1, 1999.

Hamel, F. B., "An Investigation of the Impact Properties of Vessel Steels (A Progress Report)," Proc. Div. Of Refining of American Petroleum Institute, Vol. 38, No. 3, (1958) pp. 239-257.

Lam, P. S. and R. L. Sindelar, "J-Integral Based Flaw Stability Analysis of Mild Steel Storage Tanks," in proceeding of ASME Pressure Vessel and Piping Conference, July 1999.

Marra, J. E., H. A. Abodishish, D. M. Barnes, R. L. Sindelar, H. E. Flanders, T. W. Houston, B. J. Wiersma, F. G. McNatt, Sr., C. D. Cowfer, "Savannah River Site (SRS) High Level Waste (HLW) Structural Integrity Program," in proceedings of ASME Pressure Vessel and Piping Conference, July 1995.